Rac-Dependent Signaling from Keratinocytes Promotes Differentiation of Intradermal White Adipocytes

Ueyama, Takehiko ; Sakuma, Megumi ; Nakatsuji, Mio ; Uebi, Tatsuya ; Hamada, Takeshi ; Aiba, Atsu ; Saito, Naoaki

(Citation)
Journal of Investigative Dermatology,140(1):75-84.e6

(Issue Date)
2019-07-24

(Resource Type)
journal article

(Version)
Accepted Manuscript

(URL)
https://hdl.handle.net/20.500.14094/90006131

Rac-Dependent Signaling from Keratinocytes Promotes Differentiation of Intradermal White Adipocytes

Takehiko Ueyama[1] (0000-0002-5647-3937), Megumi Sakuma[1] (0000-0001-7297-0389), Mio Nakatsuji[1] (0000-0001-6722-7400), Tatsuya Uebi[1] (0000-0001-8339-4241), Takeshi Hamada[1] (0000-0003-4921-2736), Atsu Aiba[2] (0000-0002-8192-0778) and Naoaki Saito[1] (0000-0003-3389-1367)

[1]*Laboratory of Molecular Pharmacology, Biosignal Research Center, Kobe University, Kobe 657-8501, Japan; and* [2]*Laboratory of Animal Resources, Center for Disease Biology and Integrative Medicine, Graduate School of Medicine, The University of Tokyo, Tokyo 113-0033, Japan*

Correspondence: Takehiko Ueyama, Laboratory of Molecular Pharmacology, Biosignal Research Center, Kobe University, 1-1 Rokkodai-cho, Nada-ku, Kobe 657-8501, Japan.
Tel: +81-78-803-5962, Fax: +81-78-803-5971. E-mail: tueyama@kobe-u.ac.jp

Running title: **Signaling from keratinocytes to adipocytes**

Abbreviations: *Bmp, bone morphogenic protein; dWAT, dermal white adipose tissue; DKO, double knockout; Fgf, fibroblast growth factor; K5, keratin 5 promoter; KO, knockout; PMEK, primary mouse epidermal keratinocyte; NHDF, normal human dermal fibroblast; NHEK, normal human primary epidermal keratinocyte; P, postnatal day, RT-PCR, reverse transcription-polymerase chain reaction; WAT, white adipose tissue*

ABSTRACT

Rac signaling affects numerous downstream targets *in vitro*; however, few studies have established *in vivo* levels. We generated mice with a single knockout (KO) of *Rac1* (*Keratin5 (K5)-Cre;Rac1*$^{flox/flox}$, *Rac1*-KO) and double KO of *Rac1* and *Rac3* (*K5-Cre;Rac1*$^{flox/flox}$*;Rac3*$^{-/-}$, *Rac1/Rac3*-DKO) in keratinocytes. Hairless phenotype in *Rac1*-KO mice was markedly exacerbated in *Rac1/Rac3*-DKO mice. Strikingly, *Rac1-KO* mice exhibited thinner dermal white adipose tissue, which was considerably further reduced in *Rac1/Rac3*-DKO mice. DNA microarray using primary keratinocytes from *Rac1/Rac3*-DKO mice exhibited decreased mRNA levels of *Bmp2*, *Bmp5*, *Fgf20*, *Fgf21*, *Fgfbp1*, and *Pdgfα.* Combinational treatment with BMP2 and FGF21 in culture medium, but not individual purified recombinant proteins, could differentiate 3T3-L1 fibroblasts into adipocytes, as could culture media from primary keratinocytes. Conversely, addition of anti-BMP2 or anti-FGF21 antibodies into the culture medium inhibited fibroblast differentiation. In addition, BMP2 and FGF21 treatment promoted adipocyte differentiation only of rat primary white adipocyte precursors but not rat primary brown adipocyte precursors. Furthermore, BMP2 and FGF21 treatment enhanced adipogenesis of normal human dermal fibroblasts. Notably, brown adipogenesis promoted by FGF21 was inhibited by BMP2. Thus, we propose a novel complex paracrine pathway from keratinocytes to intradermal pre-adipocytes, which functions as a Rac-dependent modulator of both white and brown adipogenesis.

INTRODUCTION

The skin, which is composed of three layers: the epidermis, dermis, and subcutaneous tissue (Koster and Roop, 2007), functions as a barrier between the organism and the environment (Proksch et al., 2008). The physiological barrier of the epidermis is established during embryogenesis and mainly localized in the cornified layer. Keratinocytes constitute approximately 90% of epidermal cells (Nestle et al., 2009). The upper part of the dermis is divided into the papillary and reticular dermis, whereas the lower part contains white adipose tissue (WAT) (Driskell et al., 2013).

Two distinct (developmentally, morphologically, and physiologically) types of WAT have been recently proposed to exist in the skin: intradermal/dermal WAT (dWAT) beneath the reticular dermis and subcutaneous WAT, which are clearly separated by a striated muscle called the panniculus carnosus in rodents (Driskell et al., 2013). Immature adipocytes in the dermis promote hair follicle cycling through Pdgfα secretion (Festa et al., 2011), demonstrating the paracrine differentiation signaling from intradermal adipocytes to the stem cells in the follicular bulge. Additionally, the possibility of reciprocal signaling from hair follicles (keratinocytes) to intradermal pre-adipocytes is suspected (Donati et al., 2014, Jahoda and Christiano, 2011); however, the detailed mechanism remains unknown. Furthermore, adipose tissues are classified into both WAT and brown adipose tissue, with beige/brite adipocytes, comprising brown adipocytes induced in the WAT, proposed as a third adipocyte type (Sanchez-Gurmaches et al., 2016). Nevertheless, the different adipocyte induction mechanisms remain unclear.

Racs (Rac1–Rac3), the best characterized members of the Rho-family of small GTPases, play fundamental roles in various cellular processes including transcriptional regulation and actin-based structure turnover (Namba et al., 2015, Ueyama, 2019). Previously, the hairless phenotype was reported in mice with Rac1 deletion (Benitah et al., 2005, Castilho et al., 2007, Chrostek et al., 2006), wherein either the keratin 5 (K5) or K14 promoter was used to effect Rac1 deletion in keratinocytes. Rac1 loss in keratinocytes prevented epidermal stem cell renewal and caused robust

commitment to stem cell differentiation, finally resulting in epidermal failure (Benitah et al., 2005). Additionally, the latter two groups reported the critical role of Rac1 in hair follicle development and maintenance. However, Rac3 function in keratinocytes and its synergistic (Nakamura et al., 2017, Vaghi et al., 2014) or antagonistic (Hajdo-Milasinovic et al., 2007) interaction with Rac1 remain unknown.

To address these issues, we generated mice with *Rac1* and *Rac3* double knockout (DKO) in keratinocytes (*K5-Cre;Rac1*$^{flox/flox}$*;Rac3*$^{-/-}$, hereafter *Rac1/Rac3*-DKO). We revealed differentiation-inducing signaling from keratinocytes to intradermal adipocytes, confirming the existence of crosstalk between epidermal keratinocytes and dWAT.

RESULTS

Expression of *Rac1*/*Rac3* in primary keratinocytes and generation of keratinocyte-specific *Rac1/Rac3*-DKO mice

Reverse transcription-polymerase chain reaction (RT-PCR) using primary mouse epidermal keratinocytes (PMEKs) obtained from wild-type mice identified *Rac1* as the predominant Rac isoform expressed in PMEKs (Figure 1a), with lesser *Rac3* expression (Figure 1b). In *K5–Cre*$^{+/-}$*;LacZ*$^{+/-}$ mice, X-gal-positive cells, representing the pattern of *K5–Cre*-driven recombination, comprised keratinocytes in the interfollicular epidermis, hair follicles, and sebaceous glands (Figure 1c). Therefore, we successfully generated mice with *Rac1-KO* and *Rac1/Rac3*-DKO in keratinocytes by crossing K5–Cre with *Rac1*$^{flox/flox}$ or *Rac1*$^{flox/flox}$*;Rac3*$^{-/-}$ mice (Figure 1d).

Rac1/Rac3-DKO mice exhibit thinner dWAT

Rac1-KO (Castilho et al., 2007, Chrostek et al., 2006) but not *Rac3*-KO mice (*Rac3*$^{-/-}$ and *Rac1*$^{flox/flox}$*;Rac3*$^{-/-}$) (Corbetta et al., 2005) exhibited a hairless phenotype (Figure 1d). *Rac3*-KO and *Rac1*$^{flox/flox}$ mice were subsequently used as controls. Around postnatal day 10 (P11–12), *Rac1*-KO mice with *Rac3* heterozygous deletion (*K5–Cre;Rac1*$^{flox/flox}$*;Rac3*$^{-/+}$) showed smaller body size compared with control (*Rac1*$^{flox/flox}$) and *Rac1*-KO mice, and an exacerbated hairless phenotype compared with *Rac1*-KO mice (Figure 1d). *Rac1/Rac3*-DKO hairless phenotype was exacerbated compared to that of *K5–Cre;Rac1*$^{flox/flox}$*;Rac3*$^{-/+}$ mice, exhibiting relatively less black color (Figure 1d). Although all control (*Rac1*$^{flox/flox}$, *Rac3*$^{-/-}$, *Rac1*$^{flox/flox}$*;Rac3*$^{-/-}$) and all except one *Rac1*-KO mice were alive at P30, *K5–Cre;Rac1*$^{flox/flox}$*;Rac3*$^{-/+}$ mice exhibited lower survival rate. Furthermore, all *Rac1/Rac3*-DKO mice died before P22 (before weaning) (Figure 2a). *Rac1/Rac3*-DKO mice exhibited significantly decreased body weight compared with *Rac3*-KO mice from P6 (Figure 2b).

To clarify the cause of early death of *Rac1/Rac3*-DKO mice, we first examined the barrier function of the skin. Control and *Rac1*-KO mice exhibited comparable toluidine blue permeability (Supplementary Figure S1a). *Rac1/Rac3*-DKO mice showed greater permeability than control (*Rac3-KO* and *Rac3-KO* plus heterozygous *Rac1-KO*) mice (Supplementary Figure S1b, c) albeit less than that in a previous reported mouse line showing no lethality (Sokabe and Tominaga, 2010), indicating that permeability did not likely underlie the early death. We then examined cells types exhibiting a functional *K5* promoter across the whole body. In *K5-Cre*$^{+/-}$*;LacZ*$^{+/-}$ mice, X-gal staining was positive in sweat glands in plantar skin, ependymal cells in the brain, epithelial cells in the esophagus and stomach, and tracheal glands, but negative in the heart, spleen, liver, and kidney (Supplementary Figure S2). Thus, no obvious *K5*-mediated KO location could be attributed to *Rac1/Rac3-DKO* early death.

Histological examination for *Rac1/Rac3*-DKO skin abnormality revealed significantly thin dermis of *Rac1/Rac3*-DKO mice compared with that of control (*Rac1*$^{flox/flox}$) and *Rac3*-KO mice from P0 (Figure 3a). Moreover, the *Rac1*-KO dermis became thinner than that of *Rac3*-KO mice at P3, and significantly thin compared with control and *Rac3*-KO dermis at P8 (Figure 3a). From P0, dermal thickness differed significantly between *Rac1-KO* and *Rac1/Rac3-DKO* mice (Figure 3a). Additionally, *Rac1*-KO and *Rac1/Rac3*-DKO mice presented hypertrophy in the epidermis and abnormal hair follicle morphology (Supplementary Figure S3).

To further examine the most severely affected dermal layer, we performed Oil Red O staining, which detects adipocytes. *Rac1/Rac3*-DKO mice exhibited significantly thinner dWAT than control and *Rac3*-KO mice from P0 (Figure 3b). *Rac1*-KO dWAT became significantly thinner than that of control and *Rac3*-KO mice at P8 (Figure 3b). These results are similar to the skin analysis findings (Figure 3a), suggesting that dWAT was the most severely affected dermal layer. Notably, the *Rac1/Rac3*-DKO dWAT was prevented from increasing its thickness from P0 (no significant difference between P0 vs P3 (P = 0.9992), P3 vs P8 (P = 0.9998), or P0 vs P8 (P =

0.8971) by two-way ANOVA, Figure 3b). Moreover, *Rac1*-KO dWAT showed significant increase between P3 and P8 ($P < 0.001$, Figure 3b) but not P0 and P3 ($P = 0.8413$).

The upper portion of hair follicles number did not significantly differ among control, *Rac3*-KO, *Rac1*-KO, or *Rac1/Rac3*-DKO mice (Figure 3c). This was consistent with reported limitation of hair follicle abnormalities to the nonpermanent part of the hair follicle in *Rac1*-KO mice (Chrostek et al., 2006), which is not associated with cyclic hair follicle growth (Fuchs, 2007).

Reduced secreted factors from *Rac1/Rac3*-DKO keratinocytes

We hypothesized that the thinner dWAT in *Rac1/Rac3*-DKO mice is associated with decreased secreted factor(s) from *Rac1/Rac3*-DKO keratinocytes. To identify such secreted factor(s), we performed DNA microarray analysis using mRNAs obtained from PMEKs of control (*Rac3*-KO) and *Rac1/Rac3*-DKO mice (Figure 4a). Among the genes decreased > 2-fold in the *Rac1/Rac3*-DKO relative to *Rac3*-KO keratinocytes (data are deposited in NCBIs GEO, GES122234), we selected six secreted factors as candidates: Bmp2, Bmp5, Fgf20, Fgf21, Fgfbp1, and Pdgfα (Figure 4a). *Bmp2*, *Fgf20*, *Fgf21*, *Fgfbp1*, and *Pdgfα* mRNA reduction was confirmed by RT-PCR using equivalent samples (Figure 4b).

3T3-L1 fibroblast differentiation to adipocytes by BMP2+FGF21

To examine the selected factor effects on adipogenesis, we firstly added purified recombinant BMP2, BMP5, FGF20, FGF21, and PDGFα proteins (purified recombinant Fgfbp1 protein was not commercially available) into the 3T3-L1 fibroblast culture medium, and examined adipogenesis by Oil Red O staining. 3T3-L1 cells supplemented with the five factors as well as those with dexamethasone, isobutyl-methylxanthine, and insulin (hereafter DMI) as a positive control, but not cells with single factor addition, demonstrated positive Oil Red O staining (Figure 4c, d). To define the secreted factor(s) involved in 3T3-L1 cell adipogenesis, we analyzed the effect of all two-factor combinations (10 patterns). Three patterns: BMP2+FGF21, BMP2+FGF20, and

PDGFα+FGF21, led to positive Oil Red O staining (Figure 4d). 3T3-L1 cell adipogenesis mediated by these three combinations was confirmed using immunoblotting for FABP4, a marker of differentiated adipocytes (Figure 4d). Adipogenesis induced by BMP2+FGF21 was also confirmed in C3H/10T1/2 mesenchymal cells, but was more difficult to achieve than that in 3T3-L1 cells (Supplementary Figure S4). Furthermore, ERK1/2 and JNK, but not p38 MAPK, phosphorylation levels were reduced in *Rac1/Rac3*-DKO compared with that in *Rac3*-KO keratinocytes (Supplementary Figure S5).

Induction of 3T3-L1 fibroblast adipogenesis via primary keratinocyte culture medium

To confirm the effects of secreted factors from keratinocytes on adipogenesis, we used the culture medium of primary keratinocytes. HuMedia-KG2-based culture medium of PMEKs cultured for > 48 h (undiluted 48-h-cultured PMEK medium, 2-fold-diluted 72-h-cultured PMEK medium using fresh Humedia-KG2, and undiluted 72-h-cultured PMEK medium) promoted increased FABP4 expression compared with that of fresh HuMedia-KG2, 24-h-cultured PMEK medium, 2-fold-diluted 48-h-cultured PMEK medium using fresh HuMedia-KG2, and Dulbecco's modified Eagle medium (DMEM) containing 10% fetal bovine serum (FBS, Figure 5a). However, we were unable to examine the effects of *Rac*-KO PMEK culture medium because of the markedly decreased number of obtained PMEKs resulting from impaired adhesion and spreading on the culture dish, even in the case of *Rac1*-KO (Supplementary Figure S6), consistent with previous reports (Chrostek et al., 2006, Hamelers et al., 2005). Next, we examined the effects of HuMedia-KG2-based normal human epidermal keratinocyte (NHEK) culture medium, focusing on the endocrine-acting FGF21 rather than the paracrine-acting FGF20 (Goetz and Mohammadi, 2013). Increased FABP4 protein expression in 3T3-L1 cells was also observed in the undiluted 48-h-cultured NHEK medium, but was inhibited by adding anti-BMP2 antibodies in the culture medium (Figure 5b). Furthermore, anti-FGF21 antibody addition ameliorated the increased FABP4 expression (Figure

5c). These results strongly supported the idea that secreted factors from keratinocytes, especially BMP2+FGF21, promote dWAT adipogenesis.

BMP2 + FGF21 induces white, but not brown, adipogenesis

Thin dWAT in *Rac1/Rac3*DKO mice and adipocyte differentiation of 3T3-L1 fibroblasts (and C3H/10T1/2 mesenchymal cells) suggested that BMP2+FGF21 induces Rac-dependent adipogenesis. To assess which types of adipocytes are induced by BMP2+FGF21, we used white and brown adipocyte precursor cells.

White adipocyte precursor treatment with BMP2+FGF21 induced strong Oil Red O positivity (Figure 6a), in the order FGF21 < BMP2 < BMP2+FGF21. This result was confirmed by FABP4 immunoblotting (Figure 6b). These findings supported that single BMP2 treatment may induce white adipogenesis, albeit not significantly; however, combinational treatment of BMP2+FGF21 markedly enhanced white adipogenesis.

In sharp contrast, brown adipocyte precursor treatment with BMP2+FGF21 did not induce increased levels of Ucp1, a brown adipocyte marker (Wang and Seale, 2016) (Figure 6c). Increased Ucp1 protein levels were only observed in brown adipocyte precursors upon DMI or FGF21, but not BMP2 or BMP2+FGF21 treatment. FGF21-mediated brown adipocyte induction is consistent with previous report (Fisher et al., 2012). Notably, BMP2 addition (BMP2+FGF21) inhibited FGF21-mediated Ucp1 induction. Overall, combinational BMP2+FGF21 treatment induced white, but not brown, adipogenesis, whereas BMP2 inhibited brown adipogenesis.

Finally, CD90-posivite normal human dermal fibroblasts (NHDFs) derived from the reticular dermis, which reportedly differentiate into adipocytes (Driskell et al., 2013, Korosec et al., 2019), were used to verify the adipogenic potential of BMP2+FGF21 toward primary fibroblasts. NHDFs were treated with or without BMP2+FGF21, according to the established protocol to differentiate fibroblasts into adipocytes (Chen et al., 2017, Korosec et al., 2019, Scott et al., 2011). Although DMI or DMI with BMP2+FGF21 afforded no adipogenesis, DMI+rosiglitazone and

DMI+rosiglitazone with BMP2+FGF21 showed adipogenesis as evaluated by FABP4 immunoblotting (Figure 6d). Notably, DMI+rosiglitazone-mediated adipogenesis was enhanced by BMP2+FGF21 addition (Figure 6d). These results suggested that: 1) adipogenesis of NHDFs induced by BMP1+FGF21 is more difficult than that observed in 3T3-L1, C3H/10T1/2, and adipocyte precursor cells; and 2) combinational BMP2+FGF21 treatment enhances adipogenesis in committed NHDFs.

DISCUSSION

In the present study we demonstrated that Rac1 and Rac3 in keratinocytes synergistically function in the development of hair follicles and dWAT. Although *Rac1/Rac3*-DKO mice exhibited mildly impaired epidermal barrier function, we consider that this is unlikely to underlie the early death of *Rac1/Rac3*-DKO mice, suggesting that the increased lethality may result from complex factors.

Epithelial-mesenchymal interactions are essential for development of the skin and its appendages, such as hair, mammary glands, and teeth (Katagiri and Watabe, 2016, Mikkola and Millar, 2006). dWAT thickness continuously cycles in accordance with the hair follicle growth cycle, being thinnest in the telogen and thickest in the anagen phase (Hansen et al., 1984, Schneider et al., 2009), which suggests the presence of signaling from hair follicles (keratinocytes) to dWAT. Several groups have reported the converse, from intradermal adipocytes to hair follicles (Chen et al., 2002, Festa et al., 2011, Jong et al., 1998). In mice, hair follicle downgrowth and morphogenesis are complete at P8 and approximately P16, respectively; this hair follicle developmental process with fully formed hair shafts is termed the “morphogenetic anagen” (Blanpain and Fuchs, 2006, Muller-Rover et al., 2001). Subsequently, the first hair follicle cycling is initiated after the catagen and telogen phases; the first actual growth phase (anagen) commences at 4 weeks after birth (Schneider et al., 2009). In our *Rac1/Rac3*-DKO mice, the skin failed to execute the final differentiation necessary to enter the hair growth cycle and increase the dWAT thickness. Although hair follicle atrophy in *Rac1/Rac3*-DKO mice may contribute to the thinner dWAT, these mice revealed the signaling from keratinocytes to intradermal pre-adipocytes, confirming the existence of reciprocal signaling/crosstalk between these cells.

Bone morphogenic proteins (Bmps), members of the transforming growth factor-β family, have been classified into several subgroups including Bmp2/4, Bmp5/6/7/8, Bmp9/10, and Bmp12/13/14 (Katagiri and Watabe, 2016). These four subgroups activate Bmp type I receptors along with Smad1, 5, and 8 (R-Smad) to regulate target gene transcription (Miyazono et al., 2010). Bmp2 and Bmp4 are generally reported to be involved in white adipogenesis, whereas Bmp7

functions in brown adipogenesis (Cristancho and Lazar, 2011, Zhang et al., 2010). Bmp4 also induces brown adipogenesis and browning of WAT (Elsen et al., 2014, Qian et al., 2013, Xue et al., 2014). Although Bmp6 was reported to induce white adipogenesis (Donati et al., 2014), Bmp6 was not identified as a downstream target of Rac in the present study. In addition, whereas *Bmp2* and *Bmp5* were detected as Rac1 downstream targets in keratinocytes, BMP5 did not induce 3T3-L1 fibroblast adipogenesis even in combination with FGF21 or FGF20. Nevertheless, we confirmed that Bmp signaling was coordinate with reduced phosphorylation levels of Smad1/5 in the *Rac1/Rac3*-DKO dWAT (Supplementary Figure S7).

The mammalian fibroblast growth factor (Fgf) family comprises 22 members grouped into intracrine-acting, endocrine-acting, and five paracrine-acting subfamilies (Goetz and Mohammadi, 2013). FGF20 and FGF21 belong to paracrine-acting and endocrine-acting subfamilies, respectively. FGF21 regulates glucose, carbohydrate, and lipid metabolism (Kurosu et al., 2007) and induces brown adipogenesis including browning in WAT (Dutchak et al., 2012, Fisher et al., 2012, Wei et al., 2012), whereas FGF20 is reportedly involved in hair follicle development (Huh et al., 2013). Periodic FGF21 and FGF 20 expression in the skin, which depends on the hair growth cycle, has been reported (Kawano et al., 2005). As an endocrine-acting Fgf, FGF21 does not appear to require Fgfbps. However, Fgf20 is a paracrine-acting Fgf; thus, Fgfbps may function in Fgf20 delivery from keratinocytes to intradermal adipocytes. In the present study, we detected decreased *Fgfbp1* mRNA levels in PMEKs; however, the binding capabilities of Fgfbp1 to Fgf20 and Fgf21 are unknown.

Notably, constitutively active mutants of Rac1 and RhoGDIβ, a Rho-family small GTPase inhibitor, could promote and prevent BMP4-induced adipogenesis in C3H10T1/2 cells, respectively (Huang et al., 2015). Additionally, signaling by the canonical Wnt, Wnt/β-catenin, in the epidermis could promote adipogenesis along with epidermal development (Blanpain and Fuchs, 2006), in which BMP2 and BMP6 (Donati et al., 2014), and FGF20 (Huh et al., 2013) were secreted from keratinocytes and hair follicles following Wnt/β-catenin signaling activation, respectively.

Furthermore, Rac1 involvement in Wnt/β-catenin signaling has been reported (Wu et al., 2008). Together, these reports and our present findings of reduced *Bmp2* and *Fgf20*/*Fgf21* mRNA levels in *Rac1/Rac3*-DKO keratinocytes support the possibility that Rac involvement in the Wnt/β-catenin signaling in keratinocytes promotes intradermal adipogenesis through Bmp2 and Fgf20/Fgf21 secretion (Wnt/β-catenin → Rac → *Bmp2* and *Fgf20*/*Fgf21*). Moreover, in support of the reduced phospho-Erk1/2 and phospho-JNK levels in *Rac1/Rac3*-DKO keratinocytes (Supplementary Figure S5), phospho-ERK1/2 → BMP2 (Chen et al., 2010) and phospho-JNK → activating transcription factor 2 (ATF2) → FGF21 pathways were reported (Solinas and Becattini, 2017, Wang et al., 2017). Bmp2 could also promote osteogenesis (Katagiri and Watabe, 2016), with low and high concentrations favoring adipogenesis and osteogenesis, respectively (Wang et al., 1993). Inhibition of Rac1 promoted Bmp2-induced osteoblastic differentiation (Onishi et al., 2013). Alternatively, Rac inhibition was conversely reported to induce adipogenesis in 3T3-L1 cells (Liu et al., 2005). These reports suggest that Rac1 activity constitutes an important element for the commitment to adipogenesis and that other factors, such as condition and cell type, may influence the adipogenesis process.

Bmp2 and Bmp4 secretion from keratinocytes has been reported (Jamora et al., 2003), along with Bmp2 signaling from dermal adipocytes to the late anagen and early telogen hair follicles in adult mice (Plikus et al., 2008) and its adipogenic effects from the anagen hair follicles to dermal myofibroblasts during wound healing (Plikus et al., 2017). We found that Bmp2 and Fgf21 secreted from keratinocytes in a Rac-dependent manner induce white adipogenesis. We also demonstrated that Fgf21, a brown adipogenesis inducer, facilitates white adipogenesis if applied in conjunction with Bmp2. Furthermore, we identified a novel brown adipogenesis-inhibitory function of Bmp2. Our findings may potentially support pro-weight gain and anti-obesity applications, through the converse modulation of white and brown adipocytes by Bmp2.

MATERIALS AND METHODS

Animals

The *Rac1*$^{flox/flox}$ (Ishii et al., 2017), *Rac1*$^{flox/flox}$*;Rac3*$^{-/-}$ (Nakamura et al., 2017), *K5*-Cre (Tarutani et al., 1997), and *CAG-CAT*^{flox}*-LacZ* mice (Sakai and Miyazaki, 1997) were described previously. *K5-Cre;Rac1*$^{flox/flox}$ and *K5-Cre;Rac1*$^{flox/flox}$*;Rac3*$^{-/-}$ mice were backcrossed to *Rac1*$^{flox/flox}$ and *Rac1*$^{flox/flox}$*;Rac3*$^{-/-}$ mice, respectively, to generate experimental animals. This study was approved by the Institutional Animal Care and Use Committee and carried out according to the Kobe University Animal Experimentation Regulation (26-03-05). Details of animal experiments are provided in Supplementary Methods.

Histochemistry

Section preparation, hematoxylin and eosin (HE) staining, and X-gal staining were performed as previously described (Ueyama et al., 2016, Ueyama et al., 2014, Ueyama et al., 2007). For Oil Red O staining, dorsal skins were dissected after transcardial perfusion with 0.9% saline solution. Sagittal cryosections, 3T3-L1 adipocytes, and rat primary adipocytes were fixed with 4% paraformaldehyde (15 min). After washing with 60% isopropanol, the fixed cryosections and cells were stained with Oil Red O solution (10 min) and photographed using a microscope equipped with a camera.

DNA microarray

DNA microarray was performed as previously described (Nakamura et al., 2017). Total RNA was extracted from P3 *Rac3*-KO and *Rac1/Rac3*-DKO PMEKs. Gene expression profiles were examined using the SurePrint G3 Mouse GE 8 × 60K Microarray kit (Agilent Technologies, Santa Clara, CA, USA).

Differentiation of 3T3-L1 fibroblasts to adipocytes by secreted factors or primary keratinocyte culture medium

3T3-L1 fibroblasts were cultured in 24-well plates using adipocyte growth medium (DMEM supplemented with MK425 (TaKaRa Bio, Shiga, Japan)). Confluent 3T3-L1 cells were treated with the following reagents supplemented to the culture medium for 5 days: DMI as a positive control; 10 ng/ml of five human recombinant secreted factors [BMP2, BMP5, FGF20, FGF21, and PDGF-AA (Wako Pure Chemicals, Osaka, Japan)]; 10 ng/ml of ten combination patterns of two secreted factors; or 10 ng/ml of a single secreted factor.

PMEK and NHEK culture media (HuMedia-KG2) were collected at 24, 28, and 72 h after incubation, then centrifuged (5,000 × *g*). Confluent 3T3-L1 culture medium was exchanged with HuMedia-KG2 plus DMI, HuMedia-KG2, PMEK supernatants (24, 48, and 72 h), PMEK supernatants diluted 2-fold using fresh HuMedia-KG2, HuMedia-KG2 with BMP2+FGF21 or BMP2+FGF20, or DMEM with 10% FBS, and incubated for 5 days. Alternately, 3T3-L1 cells were cultured for 5 days using fresh HuMedia-KG2 or supernatants 48-h-cultured with NHEK. mAb against human BMP2 or FGF21, or control mouse IgG was added to 10 μg/ml final concentration in the culture medium.

Differentiation of rat primary white and brown pre-adipocytes to adipocytes using secreted factors

Rat primary white (TaKaRa) and brown (Cosmo Bio, Tokyo, Japan) pre-adipocytes were cultured in 24-well plates using adipocyte growth medium. At confluence, culture medium was changed into adipocyte growth medium supplemented with none (as a negative control), or 200 μg/ml BMP2, FGF21, or BMP2+FGF21, and cultured for 10 days. Medium was changed once (at 5 days). As a positive control, DMI was added in the adipocyte growth medium for the first 3 days.

Differentiation of NHDFs to adipocytes using secreted factors

CD90-positive NHDFs, adult (PromoCell, Heidelberg, Germany) were cultured in 24-well plates using fibroblast growth medium. Confluent cells were firstly pre-cultured in adipocyte growth medium supplemented with or without 200 μg/ml BMP2+FGF21 for 3 days, secondly in growth medium supplemented with DMI, DMI+BMP2+FGF21, DMI+rosiglitazone (5 μM), or DMI+rosiglitazone+BMP2+FGF21 for 3 days, and finally in adipocyte growth medium (without, with, without, or with BMP2+FGF21, respectively) for 9 days (changed at every 3 days).

Antibodies, RT-PCR, PMEK isolation, cell cultures, immunoblotting, and quantitative analysis and statistics

Details are provided in Supplementary Methods.

Data availability

DNA microarray data are available in the NCBI Gene Expression Omnibus (GEO) under accession number GES122234.

Competing interests

The authors have declared that no conflicts of interests exist.

Acknowledgements

We thank Prof. Ivan de Curtis (San Raffaele Scientific Institute, Italy), and Profs. Junji Takeda and Jun-ichi Miyazaki (Osaka University, Japan) for providing the *Rac3*-KO, *K5-Cre*, and *CAG-CAT*^{flox}*-LacZ* mice, respectively. We are also thankful to Aya Shimizu, M.Sc., and Prof. Chikako Nishigori (Kobe University, Japan) for performing experiments using PMEKs and for helpful advice, respectively. This study was supported by grants from the JSPS KAKENHI program, JP17H04042 to TUeyama, JP17H04032 to NS, and JP26670124 to NS and TUeyama; a SHISEIDO Grant for Science Research, 2006 (B21 to TUeyama), a grant from the Nakatomi Foundation (NF-2009-R20 to TUeyama), grants from the Hyogo Science and Technology Association (26087 and 30075 to TUeyama); and a grant from the Naito Foundation (to TUeyama).

Author contributions

TUeyama had full access to all data in the study. TUeyama and NS take responsibility for the integrity of the data and accuracy of the data analysis. Study conceptualization: TUeyama. Supervision: NS. Methodology: TUeyama, MS, MN, and TUebi. Investigation: TUeyama, MS, MN, TUebi, and TH. Formal analysis: TUeyama, MS, and MN. Funding acquisition: TUeyama and NS. Resources: AA provided the animals. Validation: TUeyama. Visualization: TUeyama, MS, MN, and TUebi. Writing of original draft: TUeyama. Reviewing and editing of the important contents of the manuscript: all authors.

REFERENCES

Benitah SA, Frye M, Glogauer M, Watt FM. Stem cell depletion through epidermal deletion of Rac1. Science 2005;309(5736):933-5.

Blanpain C, Fuchs E. Epidermal stem cells of the skin. Annu Rev Cell Dev Biol 2006;22:339-73.

Castilho RM, Squarize CH, Patel V, Millar SE, Zheng Y, Molinolo A, et al. Requirement of Rac1 distinguishes follicular from interfollicular epithelial stem cells. Oncogene 2007;26(35):5078-85.

Chen HC, Smith SJ, Tow B, Elias PM, Farese RV, Jr. Leptin modulates the effects of acyl CoA:diacylglycerol acyltransferase deficiency on murine fur and sebaceous glands. J Clin Invest 2002;109(2):175-81.

Chen JH, Goh KJ, Rocha N, Groeneveld MP, Minic M, Barrett TG, et al. Evaluation of human dermal fibroblasts directly reprogrammed to adipocyte-like cells as a metabolic disease model. Dis Model Mech 2017;10(12):1411-20.

Chen PY, Sun JS, Tsuang YH, Chen MH, Weng PW, Lin FH. Simvastatin promotes osteoblast viability and differentiation via Ras/Smad/Erk/BMP-2 signaling pathway. Nutr Res 2010;30(3):191-9.

Chrostek A, Wu X, Quondamatteo F, Hu R, Sanecka A, Niemann C, et al. Rac1 is crucial for hair follicle integrity but is not essential for maintenance of the epidermis. Mol Cell Biol 2006;26(18):6957-70.

Corbetta S, Gualdoni S, Albertinazzi C, Paris S, Croci L, Consalez GG, et al. Generation and characterization of Rac3 knockout mice. Mol Cell Biol 2005;25(13):5763-76.

Cristancho AG, Lazar MA. Forming functional fat: a growing understanding of adipocyte differentiation. Nat Rev Mol Cell Biol 2011;12(11):722-34.

Donati G, Proserpio V, Lichtenberger BM, Natsuga K, Sinclair R, Fujiwara H, et al. Epidermal Wnt/beta-catenin signaling regulates adipocyte differentiation via secretion of adipogenic factors. Proc Natl Acad Sci U S A 2014;111(15):E1501-9.

Driskell RR, Lichtenberger BM, Hoste E, Kretzschmar K, Simons BD, Charalambous M, et al. Distinct fibroblast lineages determine dermal architecture in skin development and repair. Nature 2013;504(7479):277-81.

Dutchak PA, Katafuchi T, Bookout AL, Choi JH, Yu RT, Mangelsdorf DJ, et al. Fibroblast growth factor-21 regulates PPARgamma activity and the antidiabetic actions of thiazolidinediones. Cell 2012;148(3):556-67.

Elsen M, Raschke S, Tennagels N, Schwahn U, Jelenik T, Roden M, et al. BMP4 and BMP7 induce the white-to-brown transition of primary human adipose stem cells. Am J Physiol Cell Physiol 2014;306(5):C431-40.

Festa E, Fretz J, Berry R, Schmidt B, Rodeheffer M, Horowitz M, et al. Adipocyte lineage cells contribute to the skin stem cell niche to drive hair cycling. Cell 2011;146(5):761-71.

Fisher FM, Kleiner S, Douris N, Fox EC, Mepani RJ, Verdeguer F, et al. FGF21 regulates PGC-1alpha and browning of white adipose tissues in adaptive thermogenesis. Genes Dev 2012;26(3):271-81.

Fuchs E. Scratching the surface of skin development. Nature 2007;445(7130):834-42.

Goetz R, Mohammadi M. Exploring mechanisms of FGF signalling through the lens of structural biology. Nat Rev Mol Cell Biol 2013;14(3):166-80.

Hajdo-Milasinovic A, Ellenbroek SI, van Es S, van der Vaart B, Collard JG. Rac1 and Rac3 have opposing functions in cell adhesion and differentiation of neuronal cells. J Cell Sci 2007;120(Pt 4):555-66.

Hamelers IH, Olivo C, Mertens AE, Pegtel DM, van der Kammen RA, Sonnenberg A, et al. The Rac activator Tiam1 is required for (alpha)3(beta)1-mediated laminin-5 deposition, cell spreading, and cell migration. J Cell Biol 2005;171(5):871-81.

Hansen LS, Coggle JE, Wells J, Charles MW. The influence of the hair cycle on the thickness of mouse skin. Anat Rec 1984;210(4):569-73.

Huang HY, Zhang WT, Jiang WY, Chen SZ, Liu Y, Ge X, et al. RhoGDIbeta Inhibits Bone Morphogenetic Protein 4 (BMP4)-induced Adipocyte Lineage Commitment and Favors Smooth Muscle-like Cell Differentiation. J Biol Chem 2015;290(17):11119-29.

Huh SH, Narhi K, Lindfors PH, Haara O, Yang L, Ornitz DM, et al. Fgf20 governs formation of primary and secondary dermal condensations in developing hair follicles. Genes Dev 2013;27(4):450-8.

Ishii T, Ueyama T, Shigyo M, Kohta M, Kondoh T, Kuboyama T, et al. A Novel Rac1-GSPT1 Signaling Pathway Controls Astrogliosis Following Central Nervous System Injury. J Biol Chem 2017;292(4):1240-50.

Jahoda CA, Christiano AM. Niche crosstalk: intercellular signals at the hair follicle. Cell 2011;146(5):678-81.

Jamora C, DasGupta R, Kocieniewski P, Fuchs E. Links between signal transduction, transcription and adhesion in epithelial bud development. Nature 2003;422(6929):317-22.

Jong MC, Gijbels MJ, Dahlmans VE, Gorp PJ, Koopman SJ, Ponec M, et al. Hyperlipidemia and cutaneous abnormalities in transgenic mice overexpressing human apolipoprotein C1. J Clin Invest 1998;101(1):145-52.

Katagiri T, Watabe T. Bone Morphogenetic Proteins. Cold Spring Harb Perspect Biol 2016;8(6).

Kawano M, Komi-Kuramochi A, Asada M, Suzuki M, Oki J, Jiang J, et al. Comprehensive analysis of FGF and FGFR expression in skin: FGF18 is highly expressed in hair follicles and capable of inducing anagen from telogen stage hair follicles. J Invest Dermatol 2005;124(5):877-85.

Korosec A, Frech S, Gesslbauer B, Vierhapper M, Radtke C, Petzelbauer P, et al. Lineage Identity and Location within the Dermis Determine the Function of Papillary and Reticular Fibroblasts in Human Skin. J Invest Dermatol 2019;139(2):342-51.

Koster MI, Roop DR. Mechanisms regulating epithelial stratification. Annu Rev Cell Dev Biol 2007;23:93-113.

Kurosu H, Choi M, Ogawa Y, Dickson AS, Goetz R, Eliseenkova AV, et al. Tissue-specific expression of betaKlotho and fibroblast growth factor (FGF) receptor isoforms determines metabolic activity of FGF19 and FGF21. J Biol Chem 2007;282(37):26687-95.

Liu J, DeYoung SM, Zhang M, Zhang M, Cheng A, Saltiel AR. Changes in integrin expression during adipocyte differentiation. Cell Metab 2005;2(3):165-77.

Mikkola ML, Millar SE. The mammary bud as a skin appendage: unique and shared aspects of development. J Mammary Gland Biol Neoplasia 2006;11(3-4):187-203.

Miyazono K, Kamiya Y, Morikawa M. Bone morphogenetic protein receptors and signal transduction. J Biochem 2010;147(1):35-51.

Muller-Rover S, Handjiski B, van der Veen C, Eichmuller S, Foitzik K, McKay IA, et al. A comprehensive guide for the accurate classification of murine hair follicles in distinct hair cycle stages. J Invest Dermatol 2001;117(1):3-15.

Nakamura T, Ueyama T, Ninoyu Y, Sakaguchi H, Choijookhuu N, Hishikawa Y, et al. Novel role of Rac-Mid1 signaling in medial cerebellar development. Development 2017;144(10):1863-75.

Namba T, Funahashi Y, Nakamuta S, Xu C, Takano T, Kaibuchi K. Extracellular and Intracellular Signaling for Neuronal Polarity. Physiol Rev 2015;95(3):995-1024.

Nestle FO, Di Meglio P, Qin JZ, Nickoloff BJ. Skin immune sentinels in health and disease. Nat Rev Immunol 2009;9(10):679-91.

Onishi M, Fujita Y, Yoshikawa H, Yamashita T. Inhibition of Rac1 promotes BMP-2-induced osteoblastic differentiation. Cell Death Dis 2013;4:e698.

Plikus MV, Guerrero-Juarez CF, Ito M, Li YR, Dedhia PH, Zheng Y, et al. Regeneration of fat cells from myofibroblasts during wound healing. Science 2017;355(6326):748-52.

Plikus MV, Mayer JA, de la Cruz D, Baker RE, Maini PK, Maxson R, et al. Cyclic dermal BMP signalling regulates stem cell activation during hair regeneration. Nature 2008;451(7176):340-4.

Proksch E, Brandner JM, Jensen JM. The skin: an indispensable barrier. Exp Dermatol 2008;17(12):1063-72.

Qian SW, Tang Y, Li X, Liu Y, Zhang YY, Huang HY, et al. BMP4-mediated brown fat-like changes in white adipose tissue alter glucose and energy homeostasis. Proc Natl Acad Sci U S A 2013;110(9):E798-807.

Sakai K, Miyazaki J. A transgenic mouse line that retains Cre recombinase activity in mature oocytes irrespective of the cre transgene transmission. Biochem Biophys Res Commun 1997;237(2):318-24.

Sanchez-Gurmaches J, Hung CM, Guertin DA. Emerging Complexities in Adipocyte Origins and Identity. Trends Cell Biol 2016;26(5):313-26.

Schneider MR, Schmidt-Ullrich R, Paus R. The hair follicle as a dynamic miniorgan. Curr Biol 2009;19(3):R132-42.

Scott MA, Nguyen VT, Levi B, James AW. Current methods of adipogenic differentiation of mesenchymal stem cells. Stem Cells Dev 2011;20(10):1793-804.

Sokabe T, Tominaga M. The TRPV4 cation channel: A molecule linking skin temperature and barrier function. Commun Integr Biol 2010;3(6):619-21.

Solinas G, Becattini B. JNK at the crossroad of obesity, insulin resistance, and cell stress response. Mol Metab 2017;6(2):174-84.

Tarutani M, Itami S, Okabe M, Ikawa M, Tezuka T, Yoshikawa K, et al. Tissue-specific knockout of the mouse Pig-a gene reveals important roles for GPI-anchored proteins in skin development. Proc Natl Acad Sci U S A 1997;94(14):7400-5.

Ueyama T. Rho-Family Small GTPases: from Highly Polarized Sensory Neurons to Cancer Cells. Cells 2019;8:20.

Ueyama T, Ninoyu Y, Nishio SY, Miyoshi T, Torii H, Nishimura K, et al. Constitutive activation of DIA1 (DIAPH1) via C-terminal truncation causes human sensorineural hearing loss. EMBO Mol Med 2016;8(11):1310-24.

Ueyama T, Sakaguchi H, Nakamura T, Goto A, Morioka S, Shimizu A, et al. Maintenance of stereocilia and apical junctional complexes by Cdc42 in cochlear hair cells. J Cell Sci 2014;127(Pt 9):2040-52.

Ueyama T, Tatsuno T, Kawasaki T, Tsujibe S, Shirai Y, Sumimoto H, et al. A regulated adaptor function of $p40^{phox}$: distinct p67phox membrane targeting by $p40^{phox}$ and by $p47^{phox}$. Mol Biol Cell 2007;18(2):441-54.

Vaghi V, Pennucci R, Talpo F, Corbetta S, Montinaro V, Barone C, et al. Rac1 and rac3 GTPases control synergistically the development of cortical and hippocampal GABAergic interneurons. Cereb Cortex 2014;24(5):1247-58.

Wang EA, Israel DI, Kelly S, Luxenberg DP. Bone morphogenetic protein-2 causes commitment and differentiation in C3H10T1/2 and 3T3 cells. Growth Factors 1993;9(1):57-71.

Wang W, Seale P. Control of brown and beige fat development. Nat Rev Mol Cell Biol 2016;17(11):691-702.

Wang X, Zhu Y, Sun C, Wang T, Shen Y, Cai W, et al. Feedback Activation of Basic Fibroblast Growth Factor Signaling via the Wnt/beta-Catenin Pathway in Skin Fibroblasts. Front Pharmacol 2017;8:32.

Wei W, Dutchak PA, Wang X, Ding X, Wang X, Bookout AL, et al. Fibroblast growth factor 21 promotes bone loss by potentiating the effects of peroxisome proliferator-activated receptor gamma. Proc Natl Acad Sci U S A 2012;109(8):3143-8.

Wu X, Tu X, Joeng KS, Hilton MJ, Williams DA, Long F. Rac1 activation controls nuclear localization of beta-catenin during canonical Wnt signaling. Cell 2008;133(2):340-53.

Xue R, Wan Y, Zhang S, Zhang Q, Ye H, Li Y. Role of bone morphogenetic protein 4 in the differentiation of brown fat-like adipocytes. Am J Physiol Endocrinol Metab 2014;306(4):E363-72.

Zhang H, Schulz TJ, Espinoza DO, Huang TL, Emanuelli B, Kristiansen K, et al. Cross talk between insulin and bone morphogenetic protein signaling systems in brown adipogenesis. Mol Cell Biol 2010;30(17):4224-33.

Figure legends

Figure 1. Expression of *Rac1*/*Rac3* in primary keratinocytes and exacerbated phenotypes in *Rac1/Rac3*-DKO mice. (a, b) RT utilized P1 wild-type primary keratinocyte mRNAs. PCR with primer sets for *Rac1*, *Rac2*, and *Rac3* (30 cycles) yielded *Rac1* (358 bp) and faint *Rac3* (257 bp) bands (a). Primer sets for *Rac1*, *Rac2*, and *Rac3* at 25, 30, or 35 cycles yielded *Rac1* (455 bp) and *Rac3* (441 bp) bands at 25 and 30 cycles, respectively (b). (c) X-gal staining using *K5-Cre*$^{-/-}$*;LacZ*$^{+/-}$ and *K5-Cre*$^{+/-}$*;LacZ*$^{+/-}$ mice (P25) showed positivity in the interfollicular epidermis, hair follicle, and sebaceous gland (arrows) of *K5-Cre*$^{+/-}$*;LacZ*$^{+/-}$ mice. Scale bars: 300 μm. (d) Photographs of control, *K5-Cre;Rac1*$^{flox/flox}$ (*Rac1*$^{-/-}$, *Rac1*-KO), *Rac1*-KO with heterozygous *Rac3*-KO (*Rac1*$^{-/-}$*Rac3*$^{-/+}$) (P12, left) and control, *Rac1*$^{-/-}$*Rac3*$^{-/+}$, K5-Cre;*Rac1*$^{flox/flox}$*;Rac3*$^{-/-}$(*Rac1*$^{-/-}$*Rac3*$^{-/-}$, *Rac1/Rac3* double KO (DKO)) mice (P11, right). *Rac1/Rac3*-DKO mice exhibit strongest and exacerbated hairless phenotype. Scale bars: 10 mm.

Figure 2. Death and body weight of *Rac1/Rac3*-DKO mice. (a) Survival rate of control (n = 42: *Rac1*$^{flox/flox}$, *Rac3*-KO, *Rac1*$^{flox/flox}$*;Rac3*$^{-/-}$ = *Rac3*-KO), *Rac1*-KO (n = 12), *Rac1*$^{-/-}$*Rac3*$^{-/+}$ (n = 9), *Rac1/Rac3*-DKO (n = 9) mice. Only one *Rac1*-KO mouse died prior to P30, and all *Rac1/Rac3*-DKO mice died before P22. (b) Body weight of *Rac1/Rac3*-DKO mice (n = 11) compared with control mice (*Rac3*-KO, n = 23). Significant differences are observed from P6. **P*< 0.05, ***P* < 0.01, ****P* < 0.001 by two-way ANOVA followed by Tukey's *posthoc* test. *Rac1*-KO (n = 1) and wild-type (WT) (n = 1) are shown for reference.

Figure 3. Intradermal fat tissue thickness in *Rac1/Rac3*-DKO mice. HE staining (a and c) and Oil Red O staining (b) of 10-μm back skin sections from control, *Rac3*-KO, *Rac1*-KO, and *Rac1/Rac3*-DKO mice. (a) Skin thickness (bidirectional arrows) at P0, P3, and P8 (n = 4). Magnified images of areas indicated by squares are shown in Supplementary Figure S3b. Bars: 100 μm (P0 and P3); 300 μm (P8). (b) Oil Red O-positive intradermal fat tissue thickness (bidirectional

arrow) at P8 (stained sections shown) (n = 4). Bars: 200 μm. (c) HE-stained perpendicular sections at the level of the infundibula of the hair follicle (indicated by lines in (a) of P8) (P8, n = 3). Bars: 100 μm. *$P < 0.05$, **$P < 0.01$, ***$P < 0.001$ by two-way ANOVA with Tukey's *posthoc* test.

Figure 4. Production of *Bmp2*, *Bmp5*, *Fgf20*, *Fgf21*, and *Pdgfα* from *Rac1/Rac3*-DKO keratinocytes and induction of adipogenesis by BMP2+FGF21. (a) DNA microarray analysis using P3 *Rac3* and *Rac1/Rac3*-DKO keratinocyte mRNAs. *Fgf21*, *Fgfbp1*, *Bmp5*, *Pdgfα*, *Bmp2*, and *Fgf20* were selected as Rac-dependent keratinocyte secreted factors. RT-PCR confirmation of (a) *Rac1* mRNA levels in *Rac1/Rac3*-DKO and *Rac3*-KO keratinocytes and (b) *Fgf21*, *Fgfbp1*, *Pdgfα*, *Bmp2*, and *Fgf20* mRNA levels in *Rac1/Rac3*-DKO keratinocytes. (c, d) 3T3-L1 fibroblasts were cultured with secreted factor(s) for 5 days. Oil Red O staining induction by DMI or secreted factor recombinant protein (BMP2, BMP5, FGF20, FGF21, and PDGFα) treatment and control (without treatment) (c) or with control, BMP2, BMP5, FGF20, FGF21, PDGFα, BMP2+FGF21, BMP2+FGF20, or PDGFα+FGF21 (d) (Bars: 50 μm). Immunoblotting of 3T3-L1 lysates after recombinant secreted factor(s) treatment using an anti-FABP4 antibody. GAPDH served as a loading control.

Figure 5. Induction of adipogenesis in 3T3-L1 fibroblasts by culture medium of primary keratinocytes. (a) 3T3-L1 cells were cultured using Humedia-KG2 (with or without DMI), Humedia-KG2 cultured with primary mouse epidermal keratinocytes (PMEKs) for 24, 48, or 72 h (1/2: cultured Humedia-KG2 with PMEKs was diluted 1:1 with fresh Humedia-KG2), Humedia-KG2 with BMP2+FGF21, Humedia-KG2 with BMP2+FGF20, or Dulbecco's modified Eagle medium (+fetal bovine serum). FABP4 immunobands are visible. GAPDH served as a loading control. (b, c) 3T3-L1 cells were cultured using HuMedia-KG2 and Humedia-KG2 cultured with NHEKs for 48 h. FABP4 immunobands induced by Humedia-KG2 cultured with NHEKs are reduced by anti-BMP2 antibody, but not IgG addition (b). FABP4 immunobands are reduced by

anti-FGF21 antibody, but not IgG addition (c). GAPDH served as a loading control. sup: supernatant.

Figure 6. Induction of white or brown adipogenesis by BMP2+FGF21. White (a, b) and brown adipocyte precursors (c) cultured with adipocyte growth medium (−) plus DMI, BMP2, FGF21, or BMP2+FGF21. (a) Oil Red O-positive cells. n = 3, **P* = 0.0124, ***P* = 0.0012, ****P* = 0.0008. Bar: 5 mm. (b) White adipocyte lysate immunoblotting and FABP4 quantification. n = 4, *****P* < 0.0001. (c) Brown adipocyte lysate immunoblotting for Ucp1. n = 4, ***P* = 0.0074 (control vs. FGF21), ***P* = 0.0044 (BMP2 vs. FGF21), and ***P* = 0.0088 (BMP2+FGF21 vs. FGF21). (d) NHDFs differentiated using adipocyte growth medium plus DMI, DMI+BMP2+FGF21, DMI+rosiglitazone, or DMI+rosiglitazone+BMP2+FGF21. Lipid drops in differentiated cells (arrowheads); quantification of such cells. n = 4, *****P* < 0.0001. Bars: 100 μm. NHDF immunoblotting with FABP4 quantification. n = 4, ****P* = 0.0002. One-way ANOVA with Tukey's *posthoc* test. Immunoblotting loading control: GAPDH.

Figure 1, Ueyama et al.

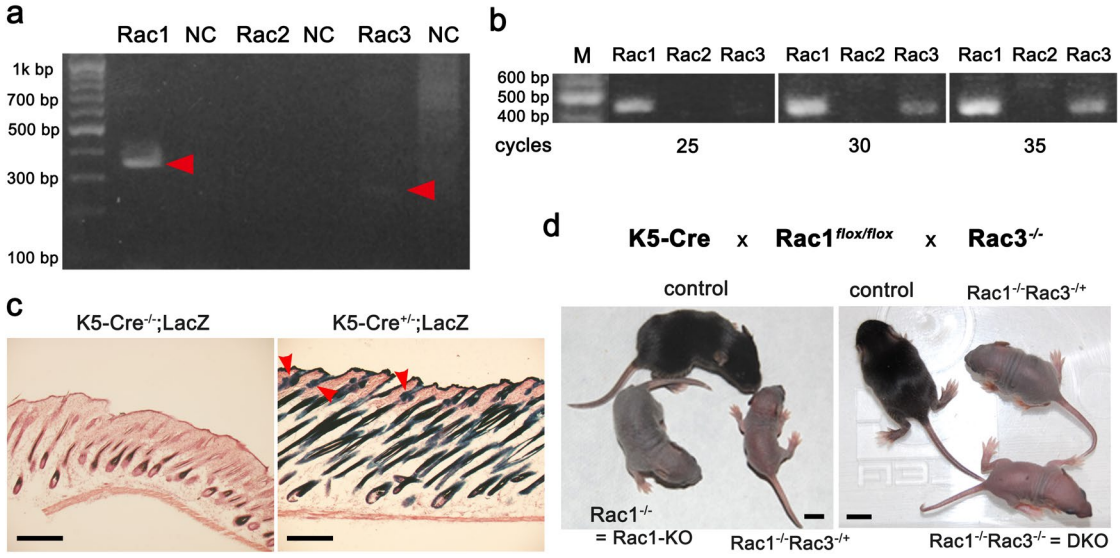

Figure 2, Ueyama et al.

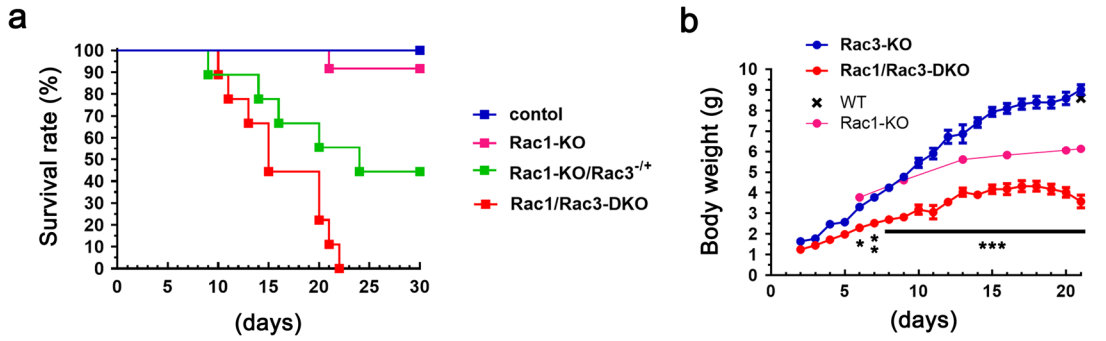

Figure 3, Ueyama et al.

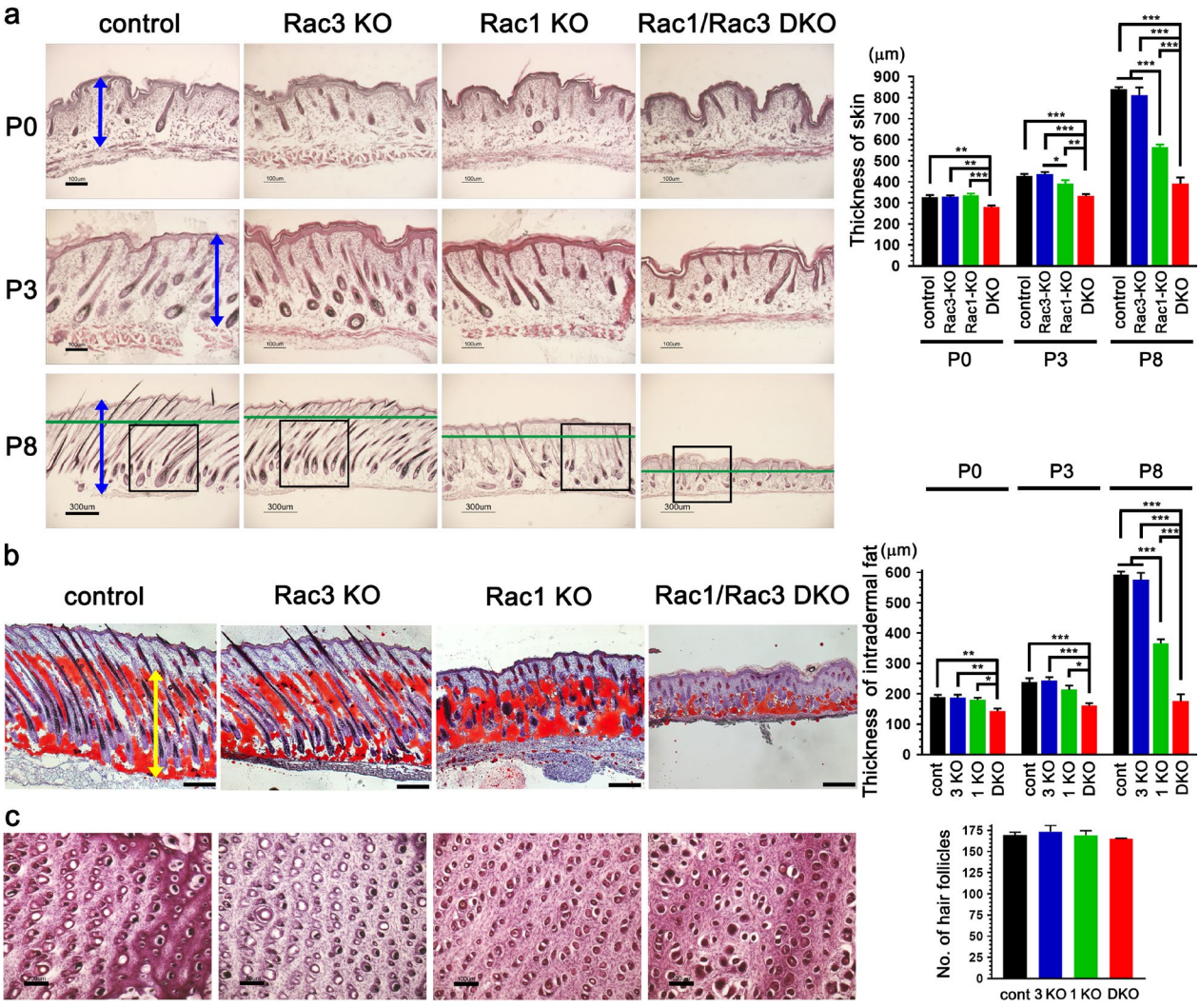

Figure 4, Ueyama et al.

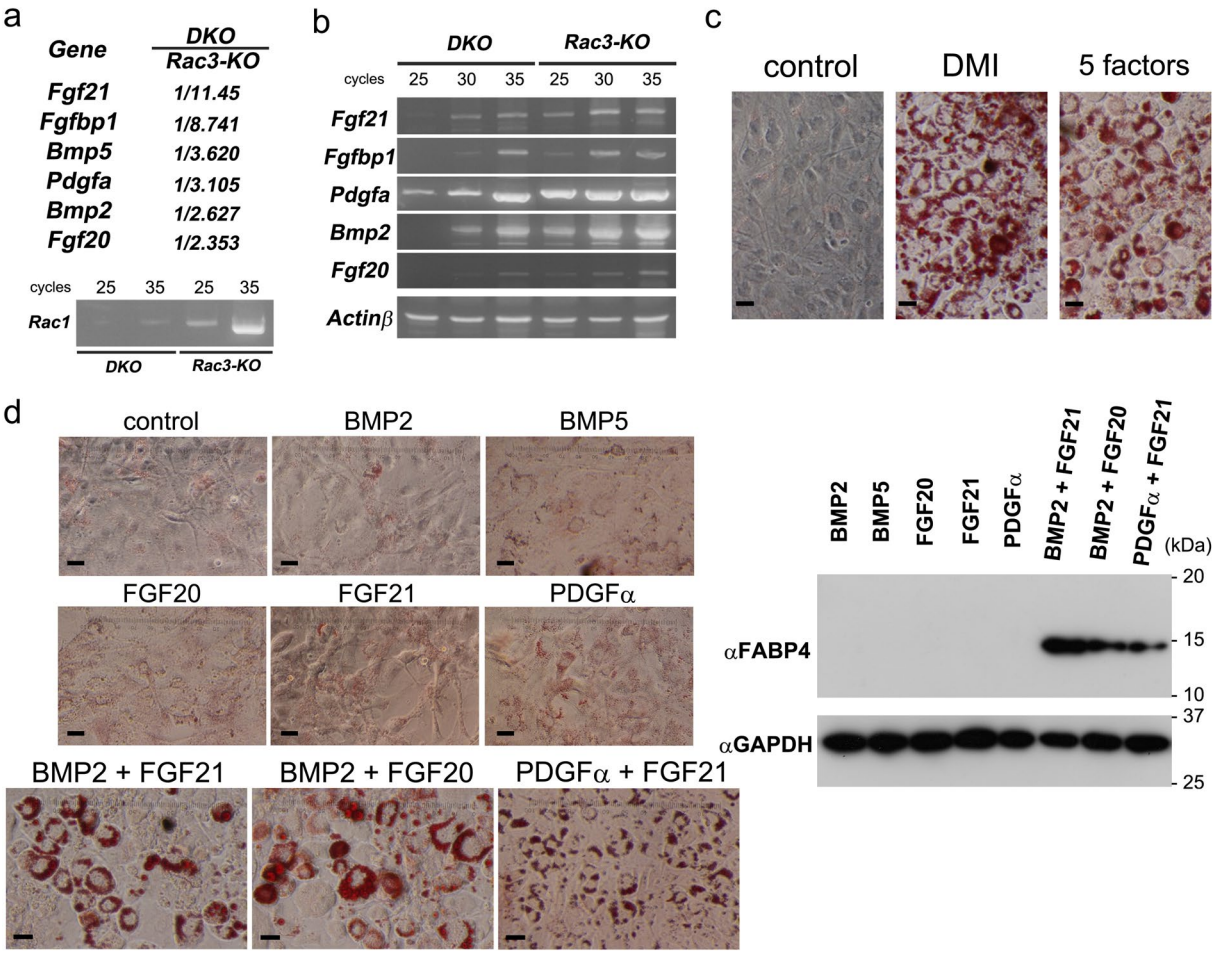

Figure 5, Ueyama et al.

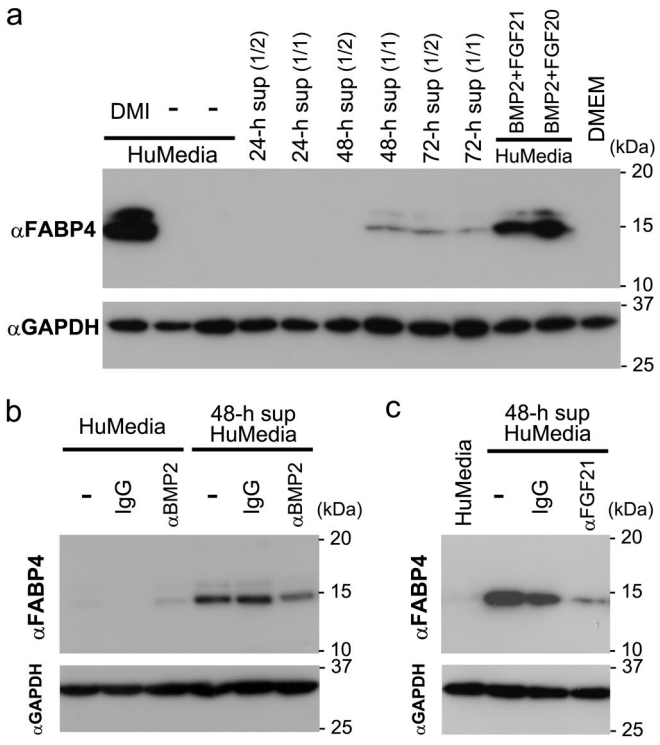

Figure 6, Ueyama et al.